

Bypassing Primary Sensory Cortices—A Direct Thalamocortical Pathway for Transmitting Salient Sensory Information

M. Liang¹, A. Mouraux² and G. D. Iannetti¹

¹Department of Neuroscience, Physiology and Pharmacology, University College London, London WC1E 6BT, UK and ²Institute of Neuroscience (IoNS), Université catholique de Louvain, B-1200 Brussels, Belgium

Address correspondence to Dr Giandomenico Iannetti, Department of Neuroscience, Physiology and Pharmacology, University College London, Medical Sciences Building, Gower Street, London WC1E 6BT, UK. Email: g.iannetti@ucl.ac.uk.

Detection and appropriate reaction to sudden and intense events happening in the sensory environment is crucial for survival. By combining Bayesian model selection with dynamic causal modeling of functional magnetic resonance imaging data, a novel analysis approach that allows inferring the causality between neural activities in different brain areas, we demonstrate that salient sensory information reaches the multimodal cortical areas responsible for its detection directly from the thalamus, without being first processed in primary and secondary sensory-specific areas. This direct thalamocortical transmission of multimodal salient information is parallel to the processing of finer stimulus attributes, which are transmitted in a modality-specific fashion from the thalamus to the relevant primary sensory areas. Such direct thalamocortical connections bypassing primary sensory cortices provide a fast and efficient way for transmitting information from subcortical structures to multimodal cortical areas, to allow the early detection of salient events and, thereby, trigger immediate and appropriate behavior.

Keywords: anterior cingulate cortex, dynamic causal modeling, functional magnetic resonance imaging, insular cortex, sensory processing

Introduction

Transient and intense sensory events reflect sudden environmental changes that require rapid and efficient processing to produce appropriate reactions. Therefore, detecting and prioritizing the processing of such salient events is a vital brain function, necessary to guarantee prompt, coherent, and adaptive behavior in an always changing sensory environment (Legrain et al. 2011). Supporting this function, a “saliency network” (SN) of cortical areas has been characterized as the neuroanatomical basis for detecting salient sensory input and prompting appropriate behavioral responses (Corbetta and Shulman 2002; Corbetta et al. 2008; Seeley et al. 2007; Iannetti and Mouraux 2010; Menon and Uddin 2010; Legrain et al. 2011; Mouraux et al. 2011).

Although several cortical areas have been suggested to be involved in saliency detection, 2 cortical structures constitute the core of this saliency network: the insular cortex (IC)—especially its anterior portion—and the anterior cingulate cortex (ACC) (Seeley et al. 2007; Iannetti and Mouraux 2010; Menon and Uddin 2010; Legrain et al. 2011; Mouraux et al. 2011). A large amount of anatomical evidence has shown that the IC and ACC, besides being heavily interconnected, have extensive connections with subcortical structures (e.g., thalamus), low-level sensorimotor areas, and high-level frontal, temporal, and parietal areas (Augustine 1985; Vogt and Pandya 1987; Vogt et al. 1987;

Augustine 1996; Wu and Kaas 2003; Medford and Critchley 2010). Consistent with this anatomical evidence, the IC and ACC are frequently coactivated in a wide range of cognitive and perceptual tasks (Dosenbach et al. 2006; Craig 2009; Medford and Critchley 2010; Torta and Cauda 2011), and they are also functionally connected at rest (Dosenbach et al. 2007; Seeley et al. 2007; Taylor et al. 2009). The IC is considered as a central integrative site for linking sensory and cognitive information (Kurth et al. 2010; Menon and Uddin 2010), playing a fundamental role in interoception and awareness (Craig 2009; Kurth et al. 2010). The ACC is thought to be involved in multiple functions, including motor, attentional, and emotional processing (Botvinick et al. 2004; Torta and Cauda 2011). All this evidence indicates that the IC and ACC could constitute a neural system adequate to detect and orient attention toward salient sensory input and to react accordingly (Seeley et al. 2007; Menon and Uddin 2010; Legrain et al. 2011; Torta and Cauda 2011). Supporting this view, the functional magnetic resonance imaging (fMRI) responses in the IC and ACC following the presentation of transient sensory stimuli correlate with the ratings of perceived stimulus saliency (Mouraux et al. 2011). Furthermore, resting-state functional connectivity studies have shown that the dorsal ACC and the insula, together with a number of other cortical and subcortical structures (e.g., the superior temporal pole and the thalamus), constitute a saliency network (Dosenbach et al. 2007; Seeley et al. 2007). This network would be responsible for identifying the most homeostatically relevant stimuli among the continuous flow of interoceptive and exteroceptive inputs and, thereby, would help the organism “decide what to do (or not to do) next” (Dosenbach et al. 2007; Seeley et al. 2007). Thus, there is converging evidence clearly indicating that the IC and ACC form a saliency network whose core function is to select salient events for additional processing and initiate appropriate control signals (Seeley et al. 2007; Iannetti and Mouraux 2010; Menon and Uddin 2010; Cauda et al. 2011; Legrain et al. 2011).

In order to understand the functional properties of this saliency network, an important question that needs to be answered is how the external sensory information flows into it. As the IC and ACC receive projections from both the thalamus and primary sensory cortices, there are at least 3 possible pathways through which sensory input could reach the saliency network: 1) the saliency network receives sensory input only after it has been processed in primary sensory cortices; 2) the saliency network receives sensory input directly from the thalamus, without preliminary processing in primary sensory cortices; and 3) the saliency network receives sensory input both directly from the thalamus and indirectly from primary sensory cortices.

Here, we tested these 3 competing hypotheses using Dynamic Causal Modeling (DCM) and Bayesian Model Selection (BMS) of the fMRI responses elicited by somatosensory, auditory and visual stimuli in the thalamus, the primary sensory cortices (primary somatosensory, auditory, and visual cortices; S1, A1, and V1), and in the 2 core regions composing the saliency network (IC and ACC). DCM is a hypothesis-driven approach to characterize the causality between the activity of different brain areas and, thereby, study how information flows in the brain (Friston et al. 2003). Combined with BMS, DCM allows testing competing hypotheses of brain connectivity, represented by different network models (Penny et al. 2010; Stephan et al. 2010), and it has been successfully applied in neuroscience (Leff et al. 2008; Liang et al. 2011). Here, we used DCM and BMS to demonstrate that salient sensory information reaches the multimodal cortical areas responsible for its detection directly from the thalamus, without being first processed in primary and secondary sensory-specific areas.

Materials and Methods

Participants

Fourteen healthy right-handed volunteers took part in the study (6 females and 8 males, aged 20–36 years). All participants gave written informed consent, and the experimental procedures were approved by the local Ethics Committee.

Sensory Stimuli and Experimental Paradigm

While lying in the scanner, participants received 4 different sensory stimuli. “Nociceptive somatosensory stimuli” were pulses of radiant heat (duration: 5 ms; beam diameter at target site: ~7 mm) generated by an infrared neodymium yttrium aluminum perovskite (Nd:YAP) laser (wavelength: 1.34 μ m; ElEn Group, Italy). The energy of the stimulus (3 ± 0.5 J) was set to elicit a clear painful pinprick sensation, related to the selective activation of $A\delta$ skin nociceptors (Bromm and Treede 1984). The stimulus was applied to the dorsum of the right foot, within the sensory territory of the superficial peroneal nerve. To prevent fatigue or sensitization of nociceptors, the laser beam was manually displaced by ~2 cm after each stimulus. “Nonnociceptive somatosensory stimuli” were constant current square-wave electrical pulses (1-ms duration; DS7A, Digitimer Ltd, UK), delivered through a pair of skin electrodes (1-cm interelectrode distance) placed at the right ankle, over the superficial peroneal nerve. For each participant, stimulus intensity (6 ± 2 mA) was adjusted to elicit a nonpainful paresthesia in the sensory territory of the nerve. The intensity of electrical stimulation was above the electrical activation threshold of $A\beta$ fibers (which convey innocuous nonnociceptive sensations) but well below the electrical activation threshold of nociceptive $A\delta$ and C fibers (Burgess and Perl 1967; Mouraux, Iannetti, et al. 2010). “Visual stimuli” consisted of a bright white disk (~9° viewing angle) displayed on the projection screen, above the right foot, for 100 ms. “Auditory stimuli” were loud, right-lateralized 800 Hz tones (0.5 left/right amplitude ratio; 50 ms duration; 5 ms rise and fall times), delivered binaurally through custom-built pneumatic earphones bored into a set of low-profile ear defenders.

The fMRI experiment consisted of a single acquisition, divided into 4 successive runs. The experimental paradigm is shown in Supplementary Figure S8. Each run consisted of a stimulation period (~8 min duration), followed by a rating period (~2 min duration). During the stimulation period, each type of stimulus was delivered 8 times (4 modalities \times 8 = 32 stimuli/period). The interstimulus interval (ISI) was 10, 13, 16, or 19 s, and each ISI was used 8 times for each modality. Both stimuli and ISIs were presented in a pseudorandom order, such that stimuli of the same modality or the same ISI were not delivered consecutively more than twice. Throughout the stimulation sequence, participants were instructed to fixate a white cross (~1.5° viewing angle) displayed at the center of the screen. During the rating period, participants were asked to rate the saliency of each stimulus modality.

This was done by adjusting the position of a cursor on 4 consecutively displayed visual-analog scales, labeled “laser,” “electric,” “visual,” and “auditory.” Each scale was displayed for 9 s. For each rating, the position of the cursor was transformed into a numerical value between 0 and 10. Left and right extremities of the scales were labeled “not salient” and “extremely salient,” respectively. The order of presentation of the 4 scales was randomized across blocks. Stimulus saliency was explained to each participant as “the ability of the stimulus to capture attention” (Mouraux and Iannetti 2009). Therefore, this subjective evaluation integrates several factors such as stimulus intensity, frequency of appearance, novelty, and its potential relevance to behavior (Kayser et al. 2005).

Blood oxygen level-dependent (BOLD) fMRI data was acquired using a 3T Varian-Siemens whole-body magnetic resonance scanner (Oxford Magnet Technology, UK). A head-only gradient coil was used with a birdcage radio frequency coil for pulse transmission and signal reception (a whole-brain gradient-echo time, 41 contiguous 3.5-mm thick slices, field of view 192 \times 192 mm, matrix 64 \times 64, with a repetition time of 3 s over 740 volumes, resulting in a total scan time of 37 min). At the end of the experiment, a T_1 -weighted structural image (1-mm thick axial slices, in-plane resolution 1 \times 1 mm) was acquired for spatial registration and the anatomical overlay of the functional data.

fMRI analysis and regions of interest selection

The fMRI data was analyzed using SPM8 (Wellcome Trust Centre for Neuroimaging, London, United Kingdom, <http://www.fil.ion.ucl.ac.uk/spm/> [date last accessed; 20 December 2011]). Data preprocessing included the following steps. For each individual data set, the first 4 volumes were discarded to allow for signal equilibration. The remaining 736 fMRI volumes were spatially realigned, normalized to the Montreal Neurological Institute space using the unified normalization-segmentation procedure implemented in SPM8, resampled to 3 \times 3 \times 3 mm³ voxel size, and spatially smoothed with an isotropic 8 mm full-width at half-maximum Gaussian kernel. Finally, the time series from each voxel were high-pass filtered (1/128 Hz cutoff) to remove low-frequency noise and signal drifts.

For each participant, first-level statistical parametric maps were obtained using a general linear model with regressors modeling the occurrence of each of the 4 types of stimuli (nociceptive somatosensory, nonnociceptive somatosensory, auditory, and visual) and their corresponding temporal and dispersion derivatives. Additional regressors were defined using the head motion parameters estimated during the fMRI volumes realignment in preprocessing. In the present study, the DCM models consisted of 2 types of brain areas: unimodal sensory areas (i.e., activated uniquely by stimuli belonging to a specific sensory modality) and multimodal sensory areas (i.e., activated by all stimuli regardless of their sensory modality). In order to identify unimodal sensory areas, 3 conventional contrast analyses were performed: unimodal somatosensory areas were identified by voxels showing significantly stronger responses to nociceptive and nonnociceptive somatosensory stimuli than to nonsomatosensory (i.e., auditory and visual) stimuli [contrast analysis: (nociceptive + nonnociceptive) > (auditory + visual)]; unimodal auditory areas were identified by contrast analysis auditory > (nociceptive + nonnociceptive + visual); unimodal visual areas were identified by contrast analysis visual > (nociceptive + nonnociceptive + auditory). We did not distinguish nociceptive-specific and nonnociceptive-specific brain areas when identifying unimodal somatosensory areas because these 2 submodalities elicit spatially indistinguishable BOLD responses (Mouraux and Iannetti 2009; Mouraux, Diukova, et al. 2010). In order to identify the multimodal sensory areas, a conjunction analysis was performed using the activation maps of all 4 sensory modalities (nociceptive somatosensory, nonnociceptive somatosensory, auditory, and visual), as implemented in SPM8 (Price and Friston 1997; Friston et al. 1999, 2005; Caplan and Moo 2004; Nichols et al. 2005). The unimodal contrast maps and multimodal conjunction maps were obtained first for each subject and then entered into a second-level analysis to obtain group level results. These group-level unimodal and multimodal statistical maps were further thresholded using $P < 0.001$ (uncorrected) and cluster > 10 voxels.

Based on group-level unimodal and multimodal sensory areas, 6 regions of interest (ROIs) (primary somatosensory [S1], auditory [A1] and visual [V1] cortices, thalamus [Th], IC, and ACC) were defined in the following steps. 1) Six anatomically defined masks were created: the somatosensory cortex mask was defined as Brodmann areas 3a, 3b, 1, and 2 and restricted to the medial wall (foot area); the auditory cortex mask was defined as Brodmann areas 41 and 42; the visual cortex mask was defined as Brodmann areas 17 and 18; the masks for thalamus, insula, and ACC were defined using the automated anatomical labeling template (Tzourio-Mazoyer et al. 2002). All masks were created only for the hemisphere contralateral to the stimulated side, i.e. the left hemisphere. 2) Unimodal and multimodal sensory areas, respectively identified by contrast and conjunction analyses, were masked by corresponding anatomical masks created in step 1, and the local maxima within each mask was obtained for each area. 3) Six ROIs (S1, A1, V1, Th, IC, and ACC) were finally created by including the 19 voxels contained within a 5-mm radius sphere centered over the local maxima. A BOLD time course was obtained for each subject and each ROI using the first eigen-vector of the time series of all the voxels contained within each ROI, adjusted for the *F* contrast of effects of interests to remove the head motion related confound, as implemented in SPM8.

Dynamic Causal Modeling

We used an effective connectivity analysis framework, DCM (Friston et al. 2003; David et al. 2008; Daunizeau et al. 2011; Friston 2009; Schuyler et al. 2010; Stephan et al. 2010) to investigate how sensory information flows from the thalamus to the cortical areas defined above. As compared with other effective connectivity analysis methods such as Granger Causal Mapping (Goebel et al. 2003) or Structural Equation Modeling (McIntosh and Gonzalez-Lima 1994; Buchel and Friston 1997), DCM is less affected by the variability of the hemodynamic response function across different brain areas and thus yields more accurate results (David et al. 2008). Furthermore, DCM is a hypothesis-driven technique (i.e., a technique used to test for a specific set of hypotheses, defined *a priori*) and is thus usually combined with BMS to test which model or which family of models provides the most likely explanation of the observed data (Penny et al. 2004, 2010; Stephan et al. 2009). DCM is featured by 3 different sets of parameters (Friston et al. 2003): 1) “intrinsic” parameters reflecting the latent connectivity between brain regions in the absence of experimental perturbations (e.g., the occurrence of a sensory stimulus), 2) “modulatory” parameters reflecting the changes in the intrinsic connectivity caused by experimental perturbations, 3) “input” parameters reflecting the driving influence on brain regions by external perturbations.

We used 2 strategies to represent the saliency network in DCM models, aiming to obtain a trade-off between model simplicity (thus achieving a better efficiency of model estimation) and model reality (thus achieving a better representation of real physiology). Based on our preliminary analyses in which we observed extremely similar results by including either IC or ACC as a single SN area in our models, a merged SN area was created by averaging the time courses of IC and ACC, to simplify the model structure in the main analysis (i.e., the first strategy; Figs 2 and 4). In this way, we were able to test the entire model space (i.e., all possible configurations of the modulatory parameters) under our hypotheses. In addition, to test the reliability of the results obtained from the simplified model structure, a more complex but also more realistic model structure was tested, including IC and ACC as 2 separate but interconnected nodes in the network (Supplementary Control Analysis A and Fig. S1a).

In this study, we hypothesized that the external perturbation generated by all sensory stimuli (i.e., the driving input) enters the model in the thalamus contralateral to the stimulated side (i.e., the receiving region), and we explored 3 possible network structures representing how the sensory information flows from the thalamus to the SN. The 3 hypotheses modeled by these 3 network structures are shown in Figure 2a. The “model structure A” represents a serial structure: sensory information flows from the thalamus (Th) to the primary sensory cortices (PSC; S1, A1, and V1) and then relays to the SN (model structure A in Fig. 2a). The “model structure B” represents a parallel structure: sensory information flows from the thalamus to both primary sensory cortices and the SN (model structure B in

Fig. 2a). The “model structure C” represents a mixed structure: sensory information flows from the thalamus to the SN via the primary sensory cortices, as well as through a direct connection from the thalamus to the SN (model structure C in Fig. 2a). As the focus of this study was to investigate how the sensory information “enters” the SN, we only modeled feed-forward connections in our main analysis, without considering backward connections (i.e., SN→PSC, SN→Th, and PSC→Th) in the main analysis. This choice was driven by the need of reducing the model complexity (but see Supplementary Control Analysis B and Figs S3 and S4 for an exploration of the contribution of backward connections in a reduced model space). Each model structure was represented by a group of single models (i.e., a model family). The single models composing a family shared the same structure of intrinsic connections but differed in how modality-specific connections (i.e., connections to or from primary sensory cortices) were modulated by external stimulation. For each of these modality-specific connections, there are 4 different possible configurations of modulatory effects exerted by external stimulation: the given connection can be modulated 1) only by stimuli of its corresponding modality, 2) only by stimuli of other modalities, 3) by stimuli of all modalities, or 4) by none of them. Similarly, there are also 4 possible configurations of modulatory parameters for the connections from the sensory cortices to the SN. Therefore, 16 models (4×4) were defined for structure A, 4 models (1×4) were defined for structure B, and 16 models (4×4) were defined for structure C. The model structure of each of the 16 single models in model family C are shown in Figure 4. The construction and estimation of the 36 single models ($16 + 4 + 16 = 36$) were performed on each individual data set, resulting in a total of 432 single models (36 models \times 12 participants) to be estimated. We did not define any modulation on the connectivity from the thalamus to the SN (Th→SN) (e.g., Fig. 4) because, in DCM, the intrinsic connectivity represents the average level of connectivity during the experiment and the modulatory connectivity represents a change of such average connectivity induced by experimental manipulations (e.g., by presentation of a certain type of stimuli). As the thalamus and the SN responded to all applied stimuli, regardless of their modality, stimulus-induced connectivity between these multimodal areas was likely to be continuously present and, hence, was unlikely to change significantly across time. Nevertheless, the inability to examine the modulation of the connectivity from the thalamus to the SN did not prevent us from testing our hypotheses because such testing relies on the intrinsic connectivity rather than on the modulatory effect. In other words, our hypothesis testing is based on the comparison between models that either include or do not include the intrinsic connectivity to allow information transfer from the thalamus to SN or from primary sensory cortices to SN. In order to test formally whether this intrinsic connectivity from the thalamus to the SN estimated in the present analysis was determined by stimulus-evoked activities in these two areas rather than by their background ongoing activities (i.e. independently of the applied stimuli), we performed a control analysis by removing the stimulus-evoked responses from the fMRI time series of SN (see Supplementary Control Analysis C).

Bayesian Model Selection

The 3 model families, representing 3 competing hypotheses, were compared using BMS. BMS uses a Bayesian framework to calculate the “model evidence” of each model. The model evidence, estimated using the negative free energy (Stephan et al. 2009), represents a trade-off between the goodness of fit and the complexity of the model, namely the number of parameters defining the model (Penny et al. 2004; Stephan et al. 2010). Here, BMS was implemented using random-effect analysis (i.e., assuming that the model structure might vary across participants) that is more robust to the presence of outliers than fixed-effect analysis (Stephan et al. 2009). Based on the estimated model evidence of each model, random effect BMS calculates the “exceedance probability,” that is, the probability of each model being more likely than any other model. When comparing model families, all models within a family were averaged using Bayesian Model Averaging (BMA), and the exceedance probabilities were calculated for each model family (Penny et al. 2010). An average model of the winning family was also

obtained at group and single-subject level. In the present study, BMS was performed on the 3 model families (to determine the best model family) as well as on the 36 single models (to determine the best single model).

Statistical Analyses of DCM Parameters

Once the best model family and the average model of the winning family obtained by BMA were calculated, statistical comparisons were performed on both intrinsic and modulatory parameters in the average model across participants. For the comparison of the intrinsic parameters, the mean amplitude of the 3 intrinsic connections from the thalamus to primary sensory cortices (i.e., Th→S1, Th→A1, and Th→V1) and the mean amplitude of the 3 intrinsic connections from the primary sensory cortices to the SN (S1→SN, A1→SN, and V1→SN) were first obtained for each participant. Then, a one-way repeated measures analysis of variance (ANOVA) was used to assess whether the strength of the 3 types of intrinsic connections (Th→PSC vs. PSC→SN vs. Th→SN) were significantly different. For the comparison of the modulatory parameters, the mean amplitude of the modulatory effects exerted by stimuli of matching modalities on the 3 connections from the thalamus to primary sensory cortices, and the mean amplitude of modulatory effects exerted by stimuli of matching modalities on the 3 connections from the primary sensory cortices to the SN were first obtained for each participant. Then, a paired two-tailed *t* test was used to assess whether the modulatory effect exerted by stimuli of matching modalities on the 2 types of connections (Th→PSC vs. PSC→SN) were significantly different.

Results

Behavioral Data

The average ratings of stimulus saliency were not significantly different across modalities ($F_{3,39} = 0.75$, $P = 0.53$, repeated measures ANOVA) and were as follows: nociceptive somatosensory: 6.1 ± 2.2 ; nonnociceptive somatosensory: 5.2 ± 2.2 ; auditory: 5.1 ± 3.0 ; visual: 5.0 ± 1.7 .

ROIs Selection

At single-subject level, 12 of 14 participants showed significant modality-specific activation in response to each of the 4 types of sensory stimuli ($P < 0.05$ uncorrected, cluster size > 10 voxels) and also conjunct activation of all stimuli ($P < 0.05$ uncorrected, cluster size > 10 voxels). Two participants did not show any significant activation and were discarded from further analyses. Six ROIs contralateral to the stimulated side were created: the 3 unimodal ROIs (S1, A1, and V1) were created based on the modality-specific activation masked with anatomically defined masks (Fig. 1*a*), and the 3 multimodal ROIs (Th, IC, and ACC) were created based on the conjunct activation masked with anatomically defined masks (Fig. 1*b*). Their spatial locations, as well as the group-level time courses of the fMRI signal following somatosensory, auditory, and visual stimulation, are shown in Figure 1.

Similarly to the previously observed correlations between the subjective saliency ratings and the fMRI responses in the IC and ACC (Mouraux et al. 2011), we found that the magnitude of the fMRI responses in the thalamus correlated significantly with the subjective ratings of saliency (Pearson's correlation coefficient; $r = 0.39$, $P = 0.006$).

DCM and BMS: Model Estimation and Selection

The group-level exceedance probabilities of all 3 families of models are shown in Figure 2*b*. Family C (representing the mixed model: sensory information is transmitted from the

thalamus to the SN both directly and indirectly) had an exceedance probability (0.981) far greater than the exceedance probabilities of families A (0.006) and B (0.013).

The estimated DCM parameters of the average model of the winning family C (Fig. 3*a*; Table 1) highlighted 3 main findings. 1) The intrinsic thalamocortical connections to primary sensory cortices (Th→S1, Th→A1, and Th→V1) and to the SN (Th→SN) were much stronger than the intrinsic corticocortical connections from the primary sensory cortices to the SN (S1→SN, A1→SN, or V1→SN). 2) External stimuli significantly modulated the thalamocortical connectivity between the thalamus and primary sensory cortices (Th→S1, Th→A1, and Th→V1) in a modality-specific way—somatosensory, auditory, and visual stimuli strongly enhanced the connectivity from the thalamus to their corresponding sensory cortices and weakly inhibited the connectivity from the thalamus to nonmatching sensory cortices. 3) The corticocortical connectivity between primary sensory cortices and the SN (S1→SN, A1→SN, or V1→SN) was not significantly modulated by external stimuli.

Each family of models was composed of several single models (A: 16, B: 4, C: 16). The group-level exceedance probabilities of each of the 36 single models (sorted according to their respective families) are shown in Figure 2*c*. Specifically, 4 single models (models 13–16; Figs 2*c* and 4) in family C had far greater exceedance probabilities (>0.22) than all other single models (≤ 0.01). These 4 single models in family C shared the common feature that the connections between the thalamus and primary sensory cortices (Th→S1, Th→A1, and Th→V1) were modulated by external stimuli in a modality-specific fashion (C13–C16 in Fig. 4), consistently with the structure of the average model described above (Fig. 3*a*).

Statistical Analysis of DCM Parameters

The one-way, repeated measures ANOVA of the strength of intrinsic connections showed a highly significant difference between the 3 types of modeled connections (Th→PSC, Th→SN, and PSC→SN: $F_{2,22} = 10.94$, $P = 0.0005$; Fig. 3*b*). Post hoc analyses (paired-sample *t* tests) showed that the intrinsic connections Th→PSC and Th→SN were significantly stronger than the intrinsic connection PSC→SN (Th→PSC vs. PSC→SN: $T_{11} = 5.04$, $P = 0.0004$; Th→SN vs. PSC→SN: $T_{11} = 3.94$, $P = 0.0023$; Fig. 3*b*). In contrast, the strength of the intrinsic connections Th→PSC and Th→SN were similar (Th→PSC vs. Th→SN: $T_{11} = 0.78$, $P = 0.45$; Fig. 3*b*).

A paired sample *t* test of modulatory parameters revealed that external stimuli exerted a significantly stronger modulatory effect on the connectivity Th→PSC as compared with the connectivity PSC→SN ($T_{11} = 3.86$, $P = 0.0027$; Fig. 3*c*).

Control Analyses

Three control analyses were performed to strengthen the above results. The first and second control analyses assessed the reliability of the results by testing the same hypotheses of the main analysis, but using more complex and realistic models in which the SN was modeled either as 2 separate but interconnected areas (IC and ACC; Supplementary Control Analysis A) or including both forward and backward connections (Supplementary Control Analysis B). Both control analyses yielded the same results obtained in the main analysis (see Supplementary Figs S1–S4). The third control analysis tested whether the identified causality between the thalamus

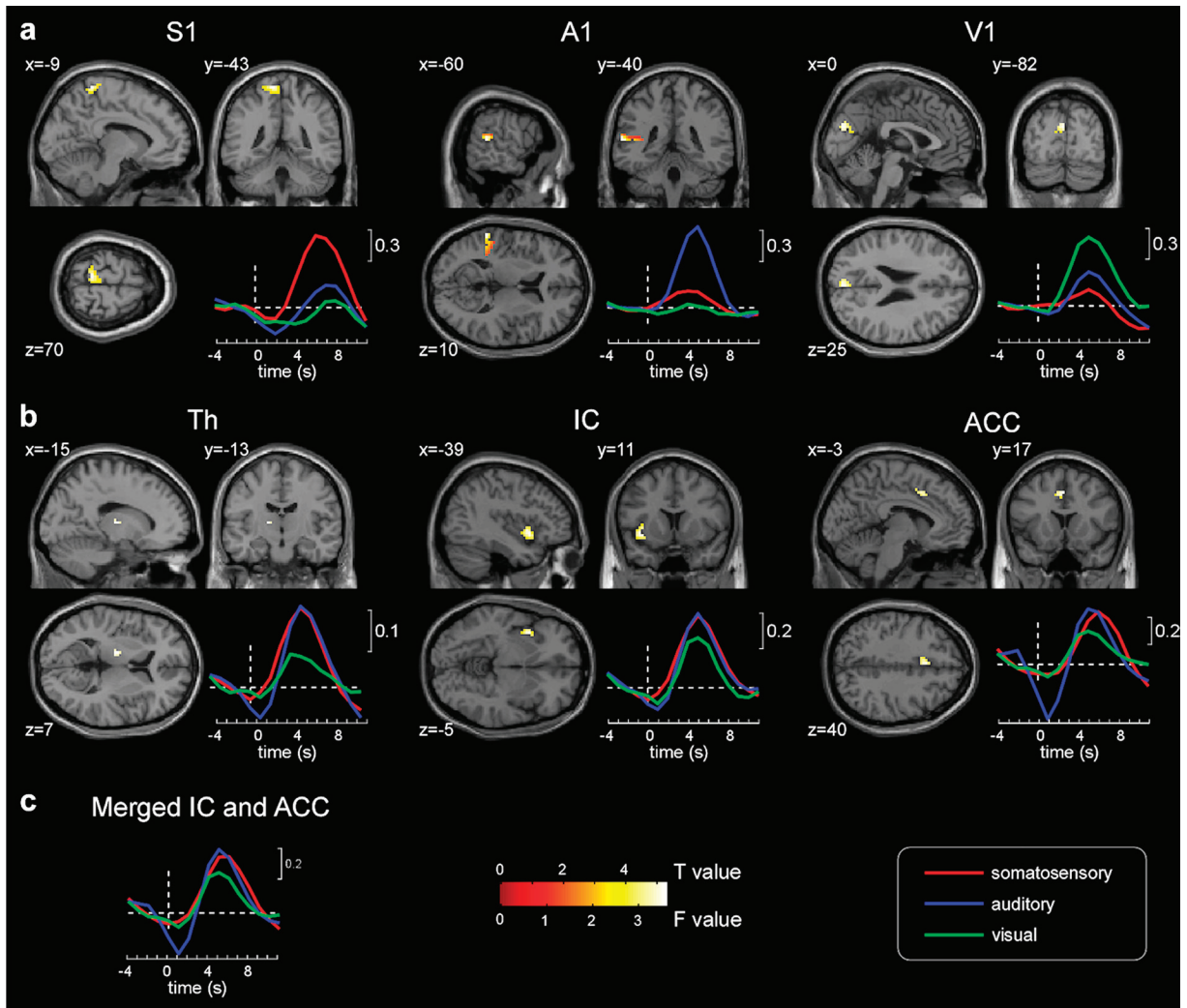


Figure 1. Spatial location and time courses of the BOLD responses in the ROIs used in the DCM analysis: primary somatosensory (S1), auditory (A1) and visual (V1) cortices, thalamus (Th), insular cortex (IC), and anterior cingulate cortex (ACC). The primary sensory cortices ROIs were identified by contrast analyses (panel *a*: S1: somatosensory > nonsomatosensory; A1: auditory > nonauditory; V1: visual > nonvisual); the color bar represents the *T* values of the corresponding contrast analysis. Th, IC, and ACC were identified by conjunction analysis of activations elicited by all types of stimuli (panel *b*); the color bar represents the *F* values of the conjunction analysis. The time courses of the BOLD signal are shown for each stimulus modality (red for somatosensory, blue for auditory, and green for visual) and for each ROI. The time course of the BOLD response in the "saliency network" was obtained by averaging the time courses of IC and ACC (panel *c*).

and SN was related to the actual transmission of stimulus-evoked sensory information from the thalamus to SN or whether it reflected background, non stimulus-related functional connectivity between these 2 structures. This was achieved by testing the same hypotheses of the main analysis after regressing out the stimulus-evoked responses from the fMRI signal time series in the SN (Supplementary Control Analysis C). This third control analysis revealed that the functional connectivity between the thalamus and SN is negligible when the stimulus-evoked fMRI responses are removed, thus demonstrating that the identified functional connectivity resulted from the transmission of stimulus-evoked sensory information from the thalamus to the SN (Supplementary Figs S5 and S6).

Discussion

Here, we used DCM and BMS to investigate the functional connectivity between the thalamus, the primary sensory cortices, and 2 brain areas—the IC and the ACC—which are

thought to play a crucial role in the detection and reaction to salient sensory information in humans. We tested 3 possible *a priori* hypotheses about how sensory input reaches the SN: 1) indirectly, passing through the thalamus and then the primary sensory cortices; 2) directly from the thalamus without being first relayed and processed within primary sensory cortices; and 3) through a combination of the above 2 pathways.

We observed 3 main results. 1) The fMRI responses elicited by somatosensory, auditory, and visual stimuli were best explained by a model including both pathways, that is, both direct thalamocortical projections from the thalamus to the SN and indirect corticocortical projections from the primary sensory cortices to the SN. 2) The intrinsic functional connectivity from the thalamus to the SN was much stronger than the intrinsic connectivity from the primary sensory cortices to the SN. 3) External stimuli significantly modulated the functional connectivity from the thalamus to the primary sensory cortices in a modality-specific manner, while they had a negligible modulatory effect on the connectivity from the

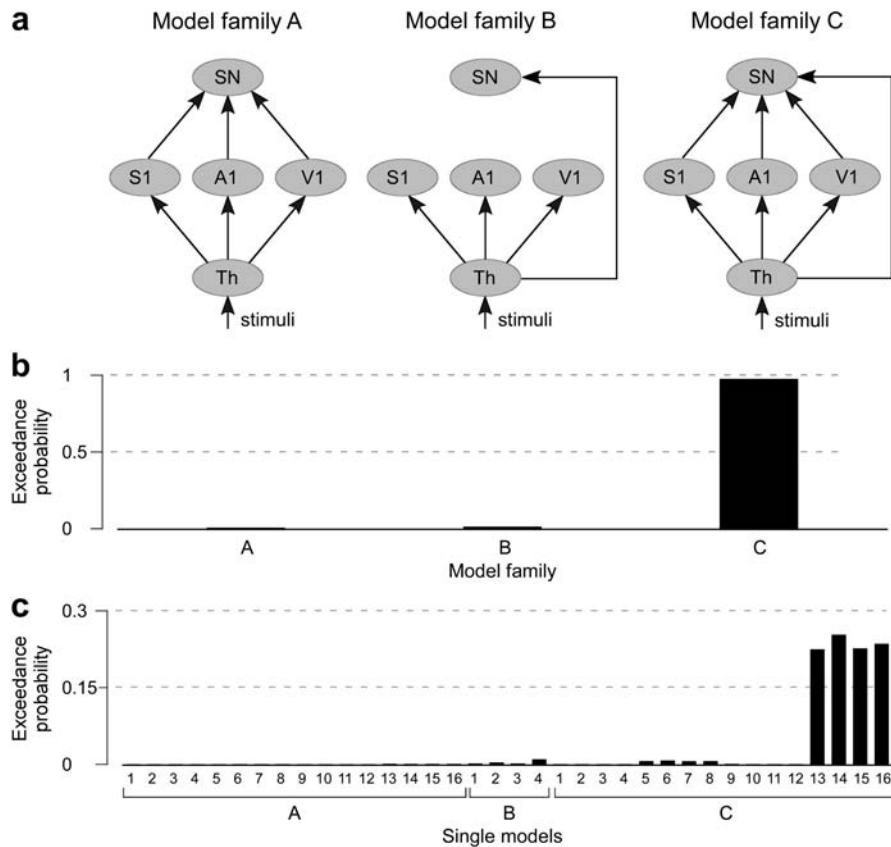


Figure 2. Structures of DCM models (a) and results of BMS on model families (b) and single models (c). Three network structures (A-C) modeled how the sensory information flows from the thalamus to the saliency network (SN) (a). Model family A: the SN receives sensory input after this has been processed in the primary sensory cortices (S1, A1, and V1). Model family B: the SN receives sensory input directly from the thalamus, without preliminary processing in primary sensory cortices. Model family C: the SN receives sensory input both directly from the thalamus and indirectly from primary sensory cortices. The black lines represent the connectivity between different brain areas; the arrows indicate the direction of the connectivity. Each model family consists of a number of single models that differ in how the connections are modulated by external stimuli. Panel b shows the exceedance probabilities of the 3 model families (A-C). The family C exceeds by far the families A and B. Panel c shows the exceedance probabilities of all 36 single models, ordered by family. Four single models belonging to family C had far greater exceedance probabilities than all other single models. Th, thalamus; S1, primary somatosensory cortex; A1, primary auditory cortex; V1, primary visual cortex; SN, saliency network.

primary sensory cortices to the SN. Altogether, these results indicate that direct input from the thalamus plays a primary role in relaying sensory information to the SN. This interpretation was also confirmed by 3 control analyses, showing that: 1) the simplified model structure used in the main analysis did not bias the findings (Supplementary Figs S1 and S2); 2) the identified thalamocortical connections to the SN were not carrying sensory information back-projected from the sensory cortices (Supplementary Figs S3 and S4); 3) the identified thalamocortical connection to the SN transmitted stimulus-evoked sensory information and did not reflect background, ongoing cortical activity (Supplementary Figs S5 and S6).

The finding that the neural activity in the thalamus causally determines the activity in the SN (Fig. 3) is supported by a large amount of anatomical evidence of direct thalamic projections to the IC and ACC in both non-human primates and humans (Jones and Leavitt 1974; Burton and Jones 1976; Mufson and Mesulam 1984; Augustine 1985, 1996; Vogt et al. 1987). More precisely, in non-human primates, the insula receives projections from several thalamic nuclei, including the centromedian nucleus, the ventral anterior nucleus, the ventral posterior inferior nucleus, and the suprageniculate-limitans nucleus (Burton and Jones 1976; Mufson and Mesulam 1984; Augustine 1985, 1996). Similarly, the dorsal part of the ACC (Brodmann

area 24, i.e., the area activated in the present study; Fig. 1b) receives direct projections from several thalamic nuclei, including the central densocellular and the intralaminar parafascicular, ventral anterior, mediodorsal, and limitans nuclei (Jones and Leavitt 1974; Vogt et al. 1987). Furthermore, the “thalamic matrix,” constituted by calbindin-positive cells that 1) are present throughout the whole thalamus without respecting the anatomical boundaries and 2) are unspecific to sensory modalities, projects diffusely to virtually all sensory and motor cortices, as well as to multimodal areas (Jones 1998, 2002). Such anatomical evidence of direct thalamocortical projections to both unimodal and multimodal cortical areas (Jones 1998; Kandel et al. 2010), together with our present finding of similarly strong intrinsic connectivity from the thalamus to SN and from the thalamus to sensory cortices (Fig. 3), are consistent with the view of a parallel processing of sensory information in the cerebral cortex (Dum et al. 2009). This parallel processing implies that at least part of the multimodal cortical responses is consequent to the convergence, already at subcortical level, of various sources of sensory information regardless of their modality (Dum et al. 2009). This is in contrast with the classical view of serial processing of sensory information, implying that sensory information is initially processed in unimodal sensory areas and then fed

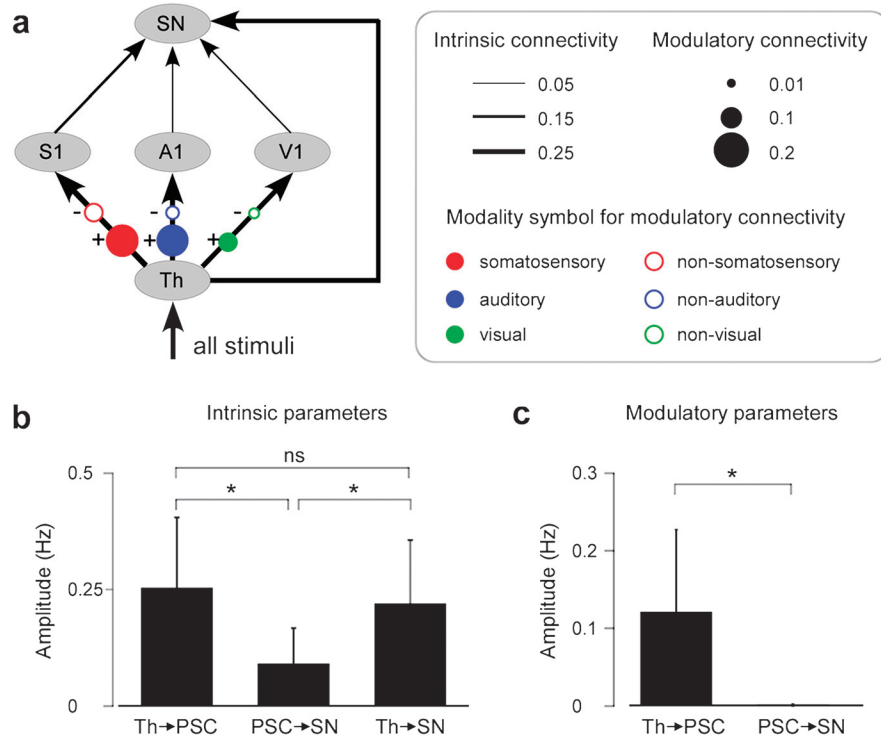


Figure 3. Estimated DCM parameters of the average model of the winning family C (a) and comparisons between the magnitudes of intrinsic (b) and modulatory (c) parameters of different types of connections. In panel a, black lines with arrows represent the intrinsic connections between brain areas; the thickness of each line represents the strength of each connection. The colored dots/circles on each connection represent the modulatory effect exerted by external stimuli; different colors represent different stimulus modalities. The size of the colored dots/circles represents the magnitude of modulatory effects, and the plus (+) and minus (−) symbols next to each dot/circle represent the direction of the modulation, with “+” indicating enhancement and “−” indicating inhibition. Modulatory effects smaller than 0.01 are not shown. Panel b shows that the intrinsic connections Th → PSC and Th → SN were significantly stronger compared with the connection PSC → SN, but there was no significant difference in the strength of the connections Th → PSC and Th → SN. Panel c shows that the applied stimuli exerted a significantly stronger modulatory effect on connection Th → PSC than on connection PSC → SN. Th, thalamus; S1, primary somatosensory cortex; A1, primary auditory cortex; V1, primary visual cortex; SN, saliency network; PSC, primary sensory cortices.

forward to multimodal areas for further higher order sensory and cognitive processing (Mesulam 1998; Kaas and Collins 2001). Thus, while the processing of sensory information transmitted from the thalamus to primary and secondary sensory cortices would constitute the basis for the ability to perceive fine sensory-discriminative features of the constant flow of sensory events arising in the surrounding world (Mountcastle 1998), the processing of sensory information transmitted from the thalamus to the SN would constitute the basis for a entirely different function, such as the immediate and effective detection and reaction to salient and potentially threatening events happening in the sensory environment (Frot et al. 2008; Legrain et al. 2011).

The aforementioned anatomical projections from the thalamus to IC and ACC, together with the evidence of a functional role of the IC and ACC in saliency detection outlined in the introduction, suggest the possibility that direct projections from the thalamus to these structures represent the anatomical substrate for the transmission of salient sensory information to the cerebral cortex. Our results clearly uphold this hypothesis: indeed, the functional connectivity Th → SN was significantly stronger than the connectivity PSC → SN, and external stimuli did not modulate the connectivity PSC → SN but only the connectivity Th → PSC (Fig. 3). Furthermore, the results of the control analysis performed by removing the stimulus-evoked responses from the fMRI time series indicate that the intrinsic connectivity from the thalamus to the SN was specifically due

to the applied sensory stimuli and did not reflect ongoing non stimulus-related background activity between these 2 structures. Indeed, the strength of the intrinsic connectivity Th → SN became negligible once the stimulus-evoked responses were removed (Supplementary Figs S5 and S6). Furthermore, the finding that not only the fMRI responses in IC and ACC (Mouraux et al. 2011) but also those in the thalamus are significantly correlated with the subjective ratings of stimulus saliency (Supplementary Fig. S7) indicate a pivotal role of the thalamus in saliency processing. In fact, the thalamus has been indicated to be part, together with the IC and ACC, of the saliency network identified in task-free resting state fMRI data, thus confirming that it has an intrinsic “functional” relationship with the IC and the ACC (Seeley et al. 2007; Cauda et al. 2011). Importantly, because of its extensive connections with cortical areas and interconnections among its various nuclei, the thalamus has been suggested not to simply relay sensory information received from peripheral receptors to the cerebral cortex but to act as an active gating mechanism filtering the flow of information to the cortex (Crick 1984; Newman 1995; McAlonan et al. 2000), selecting salient sensory information (Snow et al. 2009), and thus contributing to selective attention and perceptual awareness (Newman 1995).

The results of the present study provide, for the first time, functional evidence that saliency detection, one of the most important functions for survival, relies mainly on direct thalamocortical inputs to multimodal areas involved in this

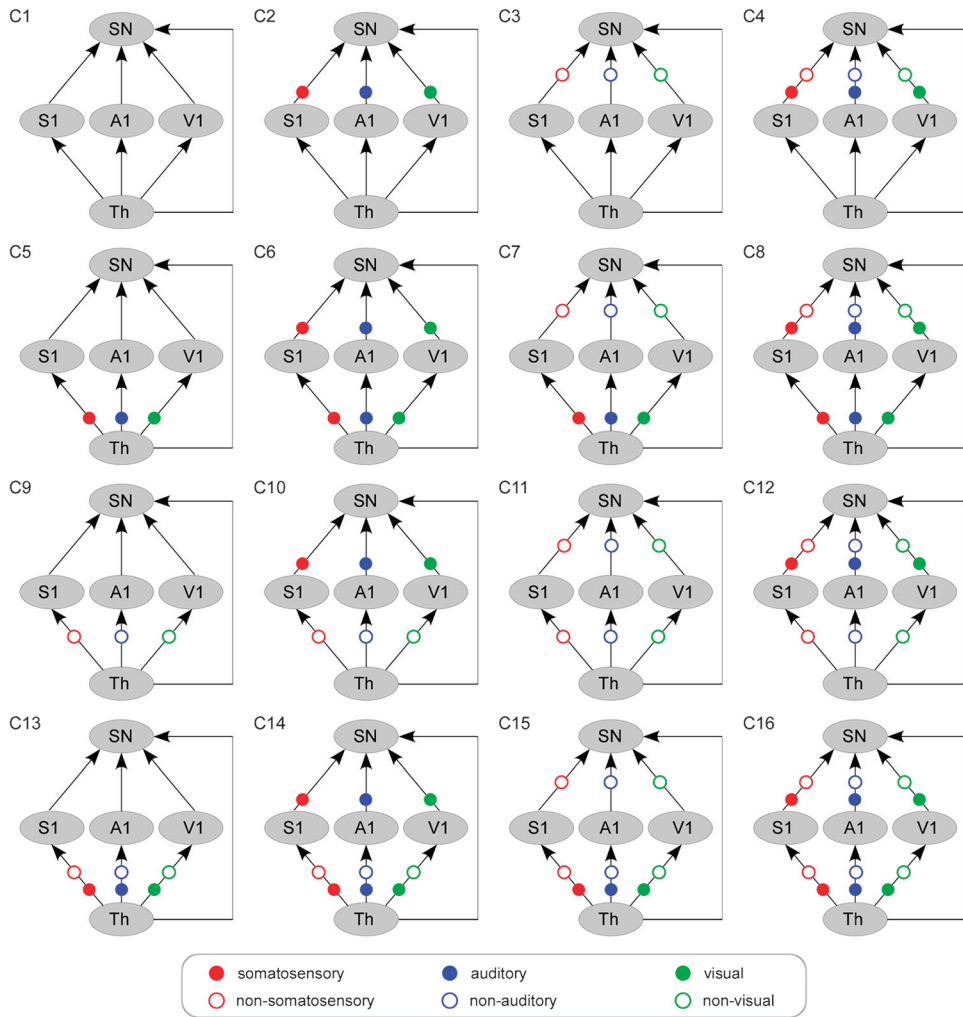


Figure 4. Structures of the 16 single models of family C. All models include 7 intrinsic connections (represented by black lines with arrows): 3 connections from the thalamus to the primary sensory cortices (S1, A1, and V1), 3 connections from the primary sensory cortices to the SN, and one direct connection from the thalamus to the SN. The arrows indicate the direction of the intrinsic connections. These 16 models differ in how the 6 connections to and from the sensory cortices are modulated by external stimulation. Such modulations are represented by colored dots/circles. Colors represent stimulus modalities. Red dots: somatosensory stimuli; red circles: nonsomatosensory stimuli (auditory and visual); blue dots: auditory stimuli; blue circles: nonauditory stimuli (somatosensory and visual); green dots: visual stimuli; green circles: nonvisual stimuli (somatosensory and auditory). Th, thalamus; S1, primary somatosensory cortex; A1, primary auditory cortex; V1, primary visual cortex; SN, saliency network.

Table 1

Magnitudes (mean \pm standard deviation) of the DCM parameters in the average model of the winning family C

Connectivity	Intrinsic parameter	Modulatory parameter by modality-matching stimuli	Modulatory parameter by modality-unmatching stimuli	Driving input
Th \rightarrow S1	$0.27 \pm 0.21^*$	$0.17 \pm 0.18^*$	$-0.05 \pm 0.07^*$	—
Th \rightarrow A1	$0.25 \pm 0.15^*$	$0.16 \pm 0.13^*$	-0.03 ± 0.05	—
Th \rightarrow V1	$0.24 \pm 0.15^*$	$0.08 \pm 0.13^*$	-0.02 ± 0.09	—
S1 \rightarrow SN	$0.13 \pm 0.13^*$	$4.0 \times 10^{-3} \pm 0.0077$	$4.56 \times 10^{-4} \pm 0.0018$	—
A1 \rightarrow SN	$0.07 \pm 0.07^*$	$-1.6 \times 10^{-3} \pm 0.0067$	$-8.02 \times 10^{-4} \pm 0.0016$	—
V1 \rightarrow SN	$0.07 \pm 0.06^*$	$-8.07 \times 10^{-4} \pm 0.0025$	$3.14 \times 10^{-4} \pm 0.0014$	—
Th \rightarrow SN	$0.22 \pm 0.14^*$	—	—	—
Inputs to Th	—	—	—	$0.26 \pm 0.21^*$

Note: *Indicates that these values are significantly different from zero ($P < 0.05$; one-sample two-tailed t test).

function. In other words, salient sensory information does not have to be processed in detail in primary and secondary sensory areas before being able to reach the SN. This hypothesis could provide an explanation for the “blindsight” phenomenon, that is, the ability of patients with cortical blindness due to a lesion of the primary visual cortex to demonstrate some responses (such as crude detection, localization, and even discrimination)

of “unseen” visual stimuli (Cowey 2010a, 2010b). Importantly, similar phenomena have been reported in other sensory modalities (Brochier et al. 1994). Blindsight is commonly interpreted as a consequence of sensory information being transmitted directly to higher order sensory cortices (e.g., areas V2 or V5 of the visual cortex) without being relayed through primary sensory cortices (e.g., area V1) (Cowey 2010a). Our

findings suggest that the blindsight phenomenon could at least in part be due to direct thalamocortical input to the SN. In support of this view, patients with blindsight typically report the occurrence of a visual stimulus as "something just happened" although they did not visually perceive it (Cowey 2010a). Such observation suggests that in those patients sensory stimuli are able to trigger responses related to the detection of saliency (through a direct activation of the SN), although the stimuli are not consciously perceived (because of the lack of activation of primary sensory cortices).

Although direct thalamocortical inputs to the SN clearly prevailed over corticocortical inputs from the primary sensory cortices (Fig. 3), the inclusion of such corticocortical connections significantly improved exceedance probabilities (model family C in Fig. 2a,b). This indicates that the primary sensory cortices contribute, albeit marginally, to the activity elicited within the SN and, hence, that their inputs may play a role in the detection of saliency. This hypothesis is consistent with the existence, in primary sensory cortices, of "saliency maps" in which a sensory input is represented not by the physical strength of a stimulus (such as the luminance of a visual stimulus) but by its saliency (such as the contrast between a visual stimulus and its surrounding stimuli) (Treue 2003). Furthermore, the transfer of sensory information from primary sensory cortices to the SN would also indicate that detailed information about the basic properties of sensory stimuli is relayed to these multimodal areas for further processing. Therefore, the SN would integrate both direct thalamic input (providing a fast but crude way to detect salient sensory events), and indirect cortical input from primary and, possibly, also associative sensory areas (providing slower but more detailed information about these events). Interestingly, the amygdala has been also demonstrated to receive sensory input both directly from the thalamus and indirectly from sensory cortical areas. Similarly, such double input has also been suggested to serve different functions: whereas the thalamic input would provide a rapid but imprecise sensory signal, the cortical input would provide a more elaborate representation of the sensory stimuli (LeDoux 2007; Sigurosson et al. 2010).

Besides the results indicating that the SN receives sensory information directly from the thalamus, we also observed that external stimuli modulated the functional connectivity from the thalamus to primary sensory cortices in a clearly modality-specific fashion: sensory stimuli enhanced the connectivity from the thalamus to their corresponding primary sensory cortex and reduced the connectivity from the thalamus to the other primary sensory cortices (Fig. 3a). The observed decrease of effective connectivity between the thalamus and primary sensory cortices by stimuli belonging to noncorresponding sensory modalities is likely to reflect an inhibition of neural activities in primary sensory cortices. Indeed, using fMRI, Laurienti et al. (2002) described a similar pattern of excitatory and inhibitory effects of sensory stimuli on different primary cortices: visual stimuli induced an activation of the visual cortex while deactivating the auditory cortex and, likewise, auditory stimuli induced an activation of the auditory cortex while deactivating the visual cortex. Such decreases in BOLD fMRI signals, likely to reflect a reduction in neural activity (Shmuel et al. 2002; Stefanovic et al. 2004; Logothetis 2008), would represent the result of the observed negative modulation exerted by nonmatching stimuli.

In conclusion, the present study provides novel and compelling evidence for a pivotal role of direct thalamocortical inputs in transmitting salient sensory information to the insula and ACC. Such direct inputs would provide a fast and efficient way for the transmission of sensory information from subcortical structures to cortical multimodal areas, to rapidly detect salient events and guide appropriate behavior.

Funding

Biotechnology and Biological Sciences Research Council (BBSRC) grant (BB/G01177X/1 to G.D.I); El.En. Group (60/10-DA to G.D.I); Royal Society University Research Fellowship (UF061613 to G.D.I). Marie Curie European Reintegration Grant (to A.M.).

Supplementary Material

Supplementary material can be found at: <http://www.cercor.oxfordjournals.org/>

Notes

The authors wish to thank Dr Chiara Sambo, Dr Elia Valentini, Miss Irene Ronga, and Miss Flavia Mancini for their insightful comments on this study. *Conflict of Interest:* None declared. The authors declare no competing financial interests.

References

- Augustine JR. 1985. The insular lobe in primates including humans. *Neurol Res.* 7:2-10.
- Augustine JR. 1996. Circuitry and functional aspects of the insular lobe in primates including humans. *Brain Res Brain Res Rev.* 22:229-244.
- Botvinick MM, Cohen JD, Carter CS. 2004. Conflict monitoring and anterior cingulate cortex: an update. *Trends Cogn Sci.* 8:539-546.
- Brochier T, Habib M, Brouchon M. 1994. Covert processing of information in hemianesthesia: a case report. *Cortex.* 30:135-144.
- Bromm B, Treede RD. 1984. Nerve fibre discharges, cerebral potentials and sensations induced by CO₂ laser stimulation. *Hum Neurobiol.* 3:33-40.
- Buchel C, Friston KJ. 1997. Modulation of connectivity in visual pathways by attention: cortical interactions evaluated with structural equation modelling and fMRI. *Cereb Cortex.* 7:768-778.
- Burgess PR, Perl ER. 1967. Myelinated afferent fibres responding specifically to noxious stimulation of the skin. *J Physiol.* 190:541-562.
- Burton H, Jones EG. 1976. The posterior thalamic region and its cortical projection in New World and Old World monkeys. *J Comp Neurol.* 168:249-301.
- Caplan D, Moo L. 2004. Cognitive conjunction and cognitive functions. *Neuroimage.* 21:751-756.
- Cauda F, D'Agata F, Sacco K, Duca S, Geminiani G, Vercelli A. 2011. Functional connectivity of the insula in the resting brain. *Neuroimage.* 55:8-23.
- Corbetta M, Patel G, Shulman GL. 2008. The reorienting system of the human brain: from environment to theory of mind. *Neuron.* 58:306-324.
- Corbetta M, Shulman GL. 2002. Control of goal-directed and stimulus-driven attention in the brain. *Nat Rev Neurosci.* 3:201-215.
- Cowey A. 2010a. The blindsight saga. *Exp Brain Res.* 200:3-24.
- Cowey A. 2010b. Visual system: how does blindsight arise? *Curr Biol.* 20:R702-R704.
- Craig AD. 2009. How do you feel-now? The anterior insula and human awareness. *Nat Rev Neurosci.* 10:59-70.
- Crick F. 1984. Function of the thalamic reticular complex: the searchlight hypothesis. *Proc Natl Acad Sci U S A.* 81:4586-4590.
- Daunizeau J, David O, Stephan KE. 2011. Dynamic causal modelling: a critical review of the biophysical and statistical foundations. *Neuroimage.* 58:312-322.

- David O, Guillemaing I, Sallet S, Rey S, Deransart C, Segebarth C, Depaulis A. 2008. Identifying neural drivers with functional MRI: an electrophysiological validation. *PLoS Biol.* 6:2683–2697.
- Dosenbach NU, Fair DA, Miezin FM, Cohen AL, Wenger KK, Dosenbach RA, Fox MD, Snyder AZ, Vincent JL, Raichle ME, et al. 2007. Distinct brain networks for adaptive and stable task control in humans. *Proc Natl Acad Sci U S A.* 104:11073–11078.
- Dosenbach NU, Visscher KM, Palmer ED, Miezin FM, Wenger KK, Kang HC, Burgund ED, Grimes AL, Schlaggar BL, Petersen SE. 2006. A core system for the implementation of task sets. *Neuron.* 50:799–812.
- Dum RP, Levinthal DJ, Strick PL. 2009. The spinothalamic system targets motor and sensory areas in the cerebral cortex of monkeys. *J Neurosci.* 29:14223–14235.
- Friston K. 2009. Causal modelling and brain connectivity in functional magnetic resonance imaging. *PLoS Biol.* 7:e33.
- Friston KJ, Harrison L, Penny W. 2003. Dynamic causal modelling. *Neuroimage.* 19:1273–1302.
- Friston KJ, Holmes AP, Price CJ, Buchel C, Worsley KJ. 1999. Multisubject fMRI studies and conjunction analyses. *Neuroimage.* 10:385–396.
- Friston KJ, Penny WD, Glaser DE. 2005. Conjunction revisited. *Neuroimage.* 25:661–667.
- Frot M, Mauguire F, Magnin M, Garcia-Larrea L. 2008. Parallel processing of nociceptive A-delta inputs in SII and midcingulate cortex in humans. *J Neurosci.* 28:944–952.
- Goebel R, Roebroek A, Kim DS, Formisano E. 2003. Investigating directed cortical interactions in time-resolved fMRI data using vector autoregressive modeling and Granger causality mapping. *Magn Reson Imaging.* 21:1251–1261.
- Iannetti GD, Mouraux A. 2010. From the neuromatrix to the pain matrix (and back). *Exp Brain Res.* 205:1–12.
- Jones EG. 1998. Viewpoint: the core and matrix of thalamic organization. *Neuroscience.* 85:331–345.
- Jones EG. 2002. Thalamic circuitry and thalamocortical synchrony. *Philos Trans R Soc Lond B Biol Sci.* 357:1659–1673.
- Jones EG, Leavitt RY. 1974. Retrograde axonal transport and the demonstration of non-specific projections to the cerebral cortex and striatum from thalamic intralaminar nuclei in the rat, cat and monkey. *J Comp Neurol.* 154:349–377.
- Kaas JH, Collins CE. 2001. The organization of sensory cortex. *Curr Opin Neurobiol.* 11:498–504.
- Kandel ER, Schwartz JH, Jessell TM. 2010. Principles of neural science. London: McGraw-Hill.
- Kayser C, Petkov CI, Lippert M, Logothetis NK. 2005. Mechanisms for allocating auditory attention: an auditory saliency map. *Curr Biol.* 15:1943–1947.
- Kurth F, Zilles K, Fox PT, Laird AR, Eickhoff SB. 2010. A link between the systems: functional differentiation and integration within the human insula revealed by meta-analysis. *Brain Struct Funct.* 214:519–534.
- Laurienti PJ, Burdette JH, Wallace MT, Yen YF, Field AS, Stein BE. 2002. Deactivation of sensory-specific cortex by cross-modal stimuli. *J Cogn Neurosci.* 14:420–429.
- LeDoux J. 2007. The amygdala. *Curr Biol.* 17:R868–R874.
- Leff AP, Schofield TM, Stephan KE, Crinion JT, Friston KJ, Price CJ. 2008. The cortical dynamics of intelligible speech. *J Neurosci.* 28:13209–13215.
- Legrain V, Iannetti GD, Plaghki L, Mouraux A. 2011. The pain matrix reloaded: a salience detection system for the body. *Prog Neurobiol.* 93:111–124.
- Liang M, Mouraux A, Iannetti GD. 2011. Parallel processing of nociceptive and non-nociceptive somatosensory information in the human primary and secondary somatosensory cortices: evidence from dynamic causal modeling of functional magnetic resonance imaging data. *J Neurosci.* 31:8976–8985.
- Logothetis NK. 2008. What we can do and what we cannot do with fMRI. *Nature.* 453:869–878.
- McAlonan K, Brown VJ, Bowman EM. 2000. Thalamic reticular nucleus activation reflects attentional gating during classical conditioning. *J Neurosci.* 20:8897–8901.
- McIntosh AR, Gonzalez-Lima F. 1994. Structural equation modeling and its application to network analysis in functional brain imaging. *Hum Brain Mapp.* 2:2–22.
- Medford N, Critchley HD. 2010. Conjoint activity of anterior insular and anterior cingulate cortex: awareness and response. *Brain Struct Funct.* 214:535–549.
- Menon V, Uddin LQ. 2010. Saliency, switching, attention and control: a network model of insula function. *Brain Struct Funct.* 214:655–667.
- Mesulam MM. 1998. From sensation to cognition. *Brain.* 121(Pt 6): 1013–1052.
- Mountcastle VB. 1998. Perceptual neuroscience: the cerebral cortex. London: Harvard University Press, XVii. p. 486.
- Mouraux A, Diukova A, Lee MC, Wise RG, Iannetti GD. 2011. A multisensory investigation of the functional significance of the “pain matrix”. *Neuroimage.* 54:2237–2249.
- Mouraux A, Iannetti GD. 2009. Nociceptive laser-evoked brain potentials do not reflect nociceptive-specific neural activity. *J Neurophysiol.* 101:3258–3269.
- Mouraux A, Iannetti GD, Plaghki L. 2010. Low intensity intra-epidermal electrical stimulation can activate Adelta-nociceptors selectively. *Pain.* 150:199–207.
- Mufson EJ, Mesulam MM. 1984. Thalamic connections of the insula in the rhesus monkey and comments on the paralimbic connectivity of the medial pulvinar nucleus. *J Comp Neurol.* 227:109–120.
- Newman J. 1995. Thalamic contributions to attention and consciousness. *Conscious Cogn.* 4:172–193.
- Nichols T, Brett M, Andersson J, Wager T, Poline JB. 2005. Valid conjunction inference with the minimum statistic. *Neuroimage.* 25:653–660.
- Penny WD, Stephan KE, Daunizeau J, Rosa MJ, Friston KJ, Schofield TM, Leff AP. 2010. Comparing families of dynamic causal models. *PLoS Comput Biol.* 6:e1000709.
- Penny WD, Stephan KE, Mechelli A, Friston KJ. 2004. Comparing dynamic causal models. *Neuroimage.* 22:1157–1172.
- Price CJ, Friston KJ. 1997. Cognitive conjunction: a new approach to brain activation experiments. *Neuroimage.* 5:261–270.
- Schuylar B, Ollinger JM, Oakes TR, Johnstone T, Davidson RJ. 2010. Dynamic Causal Modeling applied to fMRI data shows high reliability. *Neuroimage.* 49:603–611.
- Seeley WW, Menon V, Schatzberg AF, Keller J, Glover GH, Kenna H, Reiss AL, Greicius MD. 2007. Dissociable intrinsic connectivity networks for salience processing and executive control. *J Neurosci.* 27:2349–2356.
- Shmuel A, Yacoub E, Pfeuffer J, Van de Moortele PF, Adriany G, Hu X, Ugurbil K. 2002. Sustained negative BOLD, blood flow and oxygen consumption response and its coupling to the positive response in the human brain. *Neuron.* 36:1195–1210.
- Sigurosson T, Cain CK, Doyere V, LeDoux JE. 2010. Asymmetries in long-term and short-term plasticity at thalamic and cortical inputs to the amygdala in vivo. *Eur J Neurosci.* 31:250–262.
- Snow JC, Allen HA, Rafal RD, Humphreys GW. 2009. Impaired attentional selection following lesions to human pulvinar: evidence for homology between human and monkey. *Proc Natl Acad Sci U S A.* 106:4054–4059.
- Stefanovic B, Warnking JM, Pike GB. 2004. Hemodynamic and metabolic responses to neuronal inhibition. *Neuroimage.* 22:771–778.
- Stephan KE, Penny WD, Daunizeau J, Moran RJ, Friston KJ. 2009. Bayesian model selection for group studies. *Neuroimage.* 46:1004–1017.
- Stephan KE, Penny WD, Moran RJ, den Ouden HE, Daunizeau J, Friston KJ. 2010. Ten simple rules for dynamic causal modeling. *Neuroimage.* 49:3099–3109.
- Taylor KS, Seminowicz DA, Davis KD. 2009. Two systems of resting state connectivity between the insula and cingulate cortex. *Hum Brain Mapp.* 30:2731–2745.
- Torta DM, Cauda F. 2011. Different functions in the cingulate cortex, a meta-analytic connectivity modeling study. *Neuroimage.* 56:2157–2172.
- Treue S. 2003. Visual attention: the where, what, how and why of saliency. *Curr Opin Neurobiol.* 13:428–432.

- Tzourio-Mazoyer N, Landeau B, Papathanassiou D, Crivello F, Etard O, Delcroix N, Mazoyer B, Joliot M. 2002. Automated anatomical labeling of activations in SPM using a macroscopic anatomical parcellation of the MNI MRI single-subject brain. *Neuroimage*. 15:273–289.
- Vogt BA, Pandya DN. 1987. Cingulate cortex of the rhesus monkey: II. Cortical afferents. *J Comp Neurol*. 262:271–289.
- Vogt BA, Pandya DN, Rosene DL. 1987. Cingulate cortex of the rhesus monkey: I. Cytoarchitecture and thalamic afferents. *J Comp Neurol*. 262:256–270.
- Wu CW, Kaas JH. 2003. Somatosensory cortex of prosimian Galagos: physiological recording, cytoarchitecture, and corticocortical connections of anterior parietal cortex and cortex of the lateral sulcus. *J Comp Neurol*. 457:263–292.